Modulation of Respiratory Sinus Arrhythmia in Rats with Central Pattern Generator Hardware

Running title: Modulation of sinus arrhythmia with CPG hardware

Keywords: Silicon central pattern generator, neurostimulation, respiratory sinus arrhythmia, Bötzinger system

Number of pages:
Number of figures:

TOC category:

Corresponding author:
Alain Nogaret
Department of Physics
University of Bath
Claverton Down
Bath BA2 7AY, UK
A.R.Nogaret@bath.ac.uk

Julian Paton
School of Physiology and Pharmacology
Bristol Heart Institute
Medical Sciences Building
University of Bristol
Bristol, BS8 1TD, UK
Julian.F.R.Paton@bristol.ac.uk

Key points:

- First demonstration of neuromotor control in rats with neural network hardware (CPG).
- Automatic synchronization of the CPG to the rhythm of respiration as the breathing pace varies.
- Respiratory sinus arrhythmia is induced by stimulating the vagus nerve in each of the 3 phases of the respiration cycle: the inspiration phase, the early expiration phase and the late expiration phase.
- The strength of artificially induced sinus arrhythmia is found to vary depending of the timing of vagus nerve stimulation: it is strongest in the inspiration phase, a moderate strength in the second half of the expiration phase and almost inexistent if starting at the beginning of the expiration phase.

Abstract:

We report on the modulation of respiratory sinus arrhythmia in rats with central pattern generator (CPG) hardware made of silicon neurons. The neurons are made to compete through mutually inhibitory synapses to provide timed electrical oscillations that stimulate the vagus nerve at specific points of the respiratory cycle: the inspiration phase (t_1), the early expiration phase (t_2) and the late expiration phase (t_3). In this way the CPG hardware mimics the neuron populations in the medulla (Bötzinger/pre-Bötzinger complex) which under normal conditions control respiratory sinus arrhythmia (RSA). Here we stimulate the CPG hardware with the phrenic nerve (PN) while monitoring the rat heart rate (ECG), the low ventricular pressure (LVP) and the electrical activity of the central vagus nerve (VN). Neuroelectric stimulation has the effect of increasing the ventricular pressure and reducing the heart rate. The artificially induced RSA strongly depends on the timing of pulses within the breathing cycle. It is strongest when the vagus nerve is stimulated during the inspiration phase (t_1) in which case the ventricular pressure increases by a factor of 2.1 and the heart rate slows to 50% of the normal rate. The modulation is of moderate strength when stimulation is applied during the late expiration phase (t_3): the pressure increases by a factor of $\times$1.4 while the heart rate drops to 74% of the normal rate. Finally, vagus nerve stimulation produces virtually no heart modulation when it starts at the beginning of the expiration phase (t_2) and overlaps the expiration phase either partially or in its entirety. These trials show that neurostimulation by CPG hardware can provide new insights into the dynamics of the Bötzinger CPGs that couple respiration and heart rate. The CPG hardware technology also opens a new line of therapeutic possibilities for prosthetic devices that restore RSA in patients where this coupling has been lost.

I. Central Pattern Generators

Central pattern generators (CPGs) are small groups of neurons that regulate biological rhythms and coordinate motor activity. Central to rhythm generation is a pair of neurons A and B which interact through reciprocally inhibitory synapses. When neuron A fires, neuron B is blocked and vice versa. In this way neuron A and B burst out of phase with each other producing a biphasic rhythm. These neurons pairs are ubiquitous in invertebrates where they take the form of the half-centered oscillators that regulate the leech heart (Marder and Calabrese, 1996; Kristan *et al.*, 2005; Norris *et al*., 2006), the dorsal and ventral swim interneurons that control the swim motion of the tritonia and the clione (Selverston, 2010; Marder *et al.* 2005) and the triplet of pyloric neurons that produce the triphasic rhythm of the stomatogastric ganglion of the lobster (Rabinovich *et al*, 2006). In mammals, central pattern generators form hierarchies of coupled oscillators located at the base of the brain that determine motor activity such as breathing, coughing and swallowing (Shiba *et al.* 2007; Nalivaiko *et al.* 2009, Nakamura and Katakura, 1995). The central pattern generators located in the medulla (Bötzinger complex) are known to couple the rate of respiration to the heart beat with the effect of making the heart beat at a faster rate during inspiration that during expiration. This phenomenon known as respiratory sinus arrhythmia (RSA) is believed to increase blood pumping efficiency (Abdala *et al.*, 2009; Baekey *et al*. 2010; Ben-Tal *et al.* 2012; Champagnat *et al.* 2009; Fortuna *et al.*, 2009; Nicholls and Paton, 2009), reduce the risk of heart failure and possibly lower hypertension. The model proposed to describe the inhibitory and excitatory neuron populations in the Botzinger complex suggests a more complex activity whereby these CPGs provide a 3 phase stimulation of the heart within the respiration cycle (Rubin *et al*., 2009; Molkov *et al*., 2010 ; Daun *et al*., 2009; Smith *et al*., 2007). Synchronization between the cardiovascular and respiratory system has been studied in humans which evidenced phase locking intervals and phase slips between these oscillators (Schäfer *et al*. 1999; Landa and Rosenblum, 1995; Rosemblum *et al.* 2001; Rulkov *et al*., 1995). To further characterize the Bötzinger CPGs, one may stimulate the heart in each of the three phases of the model using an artificial CPG. Neurostimulation by artificial neural networks may also form the premise for novel therapies aimed at either reeducating natural central pattern generators or substituting them with prosthetic CPG implants.

II. Analogue neural hardware for neuromotor control

The interfacing of neurons with transistors is a new research front which has emerged in recent years driven by advances in microfrabrication techniques. Hybrid electronics has successfully imaged the electrical activity of individual neurons placed on transistor gates (Fromherz, 2002; Fromherz *et al*., 1991), gate arrays (Cui et al., 2001; Zheng *et al*., 2005; Patolsky *et al*., 2006)) and on graphene (Hess *et al*., 2001). Computer models of Hodgkin-Huxley neurons have been interfaced with biological neurons to understand the function of one neuron in a network. This method has been used to drive the half centered oscillator in the leech heart (Olypher *et al.*, 2006; Sorensen *et al*., 2004) and map the modes of synchronization between pairs of coupled neurons (Elson *et al*., 1998; Pinto *et al*., 2001; Varona *et al*., 2001). Although neurons models are versatile and easy to program the range of time scales associated with the Na, K, A, NaP, Ca (L), Ca (T), h and C ion channels of real neurons invariably introduces stiffness in the systems of differential equations which makes them difficult to integrate. Accurate integration of the 14 differential equations describing one such neuron is usually achieved at the cost of several minutes of computation time (Meliza *et al.*, 2012). By contrast, an artificial CPG requires neurons that respond to the stimulus accurately and in real time. Such artificial CPG therefore needs to be implemented using analogue neurons implemented in hardware. Interconnecting each neuron pair in the network with reciprocally inhibitory synapses has been predicted to allow stable spatio-temporal pulsing patterns (Rabinovich *et al*., 2001; Rabinovich *et al*., 2006; Shilnikov *et al*., 2005). These patterns repeat in a cyclic manner and within each period generate the timed pulse sequences corresponding to the bi-phasic or tri-phasic rhythms that are needed to mimic the Bötzinger CPGs..

III. Preparation of the artificial CPG

Here, we report on the first use of CPG hardware to control motor activity in rats. The network is built from 6 NaKl neurons (Mahowald and Douglas, 1991; Samardak *et al*., 2009) reciprocally interconnected with 30 (6×5) inhibitory gap synapses. In essence, the network is an analogue computer that integrates in real time the 24 (6×4) Hodgkin-Huxley equations coupled via the synaptic conductances. In addition to the synaptic currents received from the 5 other neurons, each neuron receives an external current stimulus, which in the present paper encodes the phrenic (or vagus) nerve stimulus. The network outputs the time series voltage data of representing the membrane voltages of individual neurons. To obtain biphasic rhythmic patterns it is sufficient to use a single pair of mutually inhibitory neurons. The "membrane" voltage of artificial neurons oscillates between the 0V and the 4.4V levels which corresponds to the Na action potential (+45mV) and the K action potential (-70mV) in real neurons. The voltage thresholds that open and close the Na and K ion channels were set by scaling the known biological thresholds to the 0-4.4V interval. The time constants of the Na and K gates together with the "membrane" capacitance were chosen to fit bursts of about 10-20 spikes in the inspiration phase. Given that the inspiration phase lasts 0.4s, the interval between spikes had to be in the range 20ms-40ms for a firing frequency of 25Hz - 50Hz. These are the typical frequencies obtained for a current stimulus of ~ 100μA. Our neurons have a firing threshold of 80μA and as in real neurons the firing frequency increases with increasing stimulation - up to five-fold at our maximum input current. We next performed preliminary trials of synchronization to respiration by stimulating the network with recordings of the phrenic nerve through a NI6259 DAQ card. The inhibitory synapses connecting neuron1 (N1) and neuron 2 (N2) required asymmetric conductances to obtain the biphasic rhythms that synchronize in phase and out of phase with inspiration. The synaptic conductances were adjusted by means of gate voltages.

IV. Preparation of live experiments

In live experiments, the CPG received input from the phrenic nerve and produced voltage oscillations that were used to stimulate the vagus nerve (Figure 1a). The raw phrenic signal consists of fast voltage oscillations during the inspiration phase that require amplification, rectification, smoothing and conversion to a current to stimulate the CPG. The processing is done electronically in the series of steps depicted in Figure 1a. The raw signal (rms amplitude = 70μV) is first amplified 10,000 times by the narrow band pre-amplifier that filters out noise. The signal is then amplified by a second amplifier stage that has gain tuneable in the 1-20 range and whose purpose is to finely adjust the amplitude of the stimulus relative to the firing threshold of neuron 1. This onset corresponds to the opening of the Na channel gate (1.353V). After amplification, the signal still oscillates about 0V. The next processing stage rectifies and smoothes the signal with a diode bridge and RC integrator with time constant of 1ms. The typical waveform of the rectified and integrated phrenic signal is shown in Figure 1c. This voltage (V_{ph}) is then converted into a current (I_{ph}) by a transconductance differential amplifier performing the function $I_{ph} = GV_{ph}$ where G=0.1mS. The current I_{ph} is then injected into N1 - the leftmost neuron in the lower part of Figure 1b. N1 or N2 then modulate the cardiac rhythm through stimulation of the vagus nerve (VN). The neuron may be directly connected to the vagus nerve as in most experiments the input impedance of the vagus nerve is larger than the leakage resistance in our artificial neurons (10kΩ). Changes in conductivity of the Ringer bath may however cause the impedance of the stimulating electrode to drop below 10kΩ decreasing the amplitude of neuron spikes. To guard against attenuation of the output signal, we lower the output impedance of the neuron by fitting an emitter follower amplifier between the stimulating neuron and the vagus nerve.

This circuit was designed to provide 3 phase stimulation, namely to selectively excite the vagus nerve during inspiration (t_1), early expiration (t_2) and late expiration (t_3) as shown in Figure 1c. When excited by the phrenic input, N1 and N2 fire during phase 1 and phases 2+3 respectively. To stimulate phase 3 only, we introduce a time delay τ to slow the rise of the current stimulating neuron 2 (Figure 1a). In this way, we are able to tune the timing of N2 by controlling the moment at which the input current reaches the 80 μA firing threshold. To stimulate phase 2 only, we substitute the phrenic nerve to the central

vagus nerve as input to N1. This is because the vagus nerve peaks in phase 2 hence can trigger the firing of N1 in this time interval. Although the amplitude of neuron oscillations (4.4V) is large compared to the action potentials in the vagus nerve (-70mV $\rightarrow$ +40mV -) a large fraction of this signal is dissipated through resistive losses in the envelope of the vagus nerve. Unlike in current clamp experiments where current is applied across the membrane, vagus nerve stimulation is mostly external hence requires stimulating voltages of about 4V (check!).

V. Results

We first studied the motor patterns induced by exciting the vagus nerve during the inspiration phase t_1 (Figure 2). Strong artificial RSA is seen in the ventricular pressure (LVP) in the early expiration phase where the amplitude of pressure oscillations increases by factor 2.1 whilst the interval between heart beats doubles from 0.2s to 0.4s (Figure 2a). This artificially induced sinus arrhythmia is seen to cover the duration of the early expiration phase (t_2) before the heart rate rapidly returns to normal in phases 3 and 1. Delayed sinus arrhythmia is observed in the two rats we have studied, see panels (a) and (b). In panel (b) the injection of vasopressin has the effect of increasing the breathing rate and making the ventricular pressure peak around 3937s. Here again the interval between heart beats almost doubles from 0.19s in region 1 to 0.34s in region 2. Figure 2b shows that N1 remains perfectly synchronized to the phrenic input throughout the vasopressin drive.

In Figure 3, the vagus nerve is now stimulated by the N2 during the whole duration of the expiration phase (t_2+t_3). The firing of N1 is triggered by the phrenic signal whilst N1 and N2 synchronize out of phase (Figure 3b). In this situation and although the firing of N2 is sustained over a large period of time, the induced modulation is weak and shows phase slips: the heart occasionally misses a beat at random times (Figure 3a, red arrows). The second rat shows a similarly weak modulation in the LVP trace. The most pronounced dips however appear at more regular locations at the beginning of the late expiration phase.

Figure 4 shows the effect of stimulating the vagus nerve over a short time interval at the beginning of the expiration phase. For this we trigger the firing of N1 using the signal from the central vagus nerve as an

input. This is because the VN signal peaks immediately after the inspiration phase hence suits this purpose. The resulting sinus arrhythmia is hardly detectable when the spike burst is so narrow as to only be confined to phase 2 (Figure 4a). This is similar to the results in Figure 3. If by contrast, the spike bursts become broad enough to overlap the inspiration phase (Figure 4b), the strong RSA described in Figure 2 is reappears. The amplitude of the artificially modulated pressure oscillations increases by a factor of 3 while the interval between heart beats doubles from 0.15s to 0.33s. It therefore appears that stimulating the vagus nerve at the beginning of the expiration phase and for no matter how long the stimulation lasts has no effect on RSA. This is especially remarkable given that more energy is expended stimulating the expiration phase (Figure 3) which lasts 7 times more than the inspiration phase (Figure 2). From the above results it would appear that RSA cannot be modulated by stimulating the vagus nerve in the expiration phase. However this is not the case. It appears that when the stimulation is delayed until late in the expiration phase RSA can be artificially induced. Figure 5 reports the effect of applying the spike bursts in the second half of the expiration phase. This was achieved by delaying the raise of the current stimulation N2. Surprisingly, a moderate sinus arrhythmia is observed characterized by a small but regular increase of the interval between heart beats from 0.2s to 0.27s (Figure 5a). When electrical stimulation is applied over shorter intervals at the end of the 3rd phase, the RSA modulation exists but is too feeble to quantify.

Finally Figure 6 shows the natural respiratory sinus arrhythmia observed when the CPG feedback loop of Figure 1 is disconnected.

VI. Interpretation

The general conclusions that can be drawn from this study are that electrical stimulation of the vagus nerve has the effect of decreasing the heart rate while increasing the heart pressure. Hence, the vagus nerve can be said to have inhibitory action on the heart rate. The artificially induced RSA during the inspiration phase may therefore be so strong because stimulation from the Bötzinger CPGs is absent during this period. The lack of vagus nerve stimulation during inspiration can explain why RSA makes the heart run faster during the inspiration phase than in the expiration phase and not vice-versa. The

absence of any artificially induced RSA in the expiration phase would similarly be because the Bötzinger CPGs are actively stimulating the vagus nerve in this period slowing down the heart rate. Further stimulation by our CPG would only add a perturbation to the stimulation from Bötzinger CPGs. As perturbation the CPG behaves as an additional oscillator that competes with the respiration oscillator to synchronize with the heart beat. Without any external perturbation, respiration and the cardiovascular system form two oscillators which are known to be coupled (Figure 6). This coupling takes the form of either phase or frequency locking. The effect of the CPG perturbation is to introduce the phase slips sown as the red arrows in Figure 3. Such behaviour is known to occur when the synchronization region between two oscillators is being reduced by an external perturbation. Schäfer et al. (Schäfer et al., 1999) have modeled the heart as a noisy van der Pol oscillator whose natural oscillation frequency is modulated by respiration. In such system, noise is the perturbation. Its effect is to narrow the region of synchronization allowing phase slips to occur. Since, here, the perturbation is not noise but neuron oscillations, the phase slips could simply indicate that the neuron oscillator competes with respiration to synchronize with the heart beat.

Lastly, the resurgence of heart sensitivity to vagus nerve stimulation late in the expiration phase supports the model of a tri-phasic action of the Bötzinger CPGs. This also suggests that the Bötzinger CPGs provide less excitation of the vagus nerve in the second half of the expiration phase.

In summary we have shown that an artificial CPG can be used to induce artificial respiratory sinus arrhythmia. The modulation of the heart output is most effective in the inspiration phase and to a lesser extent in the late expiration phase while no action is observed in the first half of the expiratory phase. This suggests that RSA is due to Bötzinger CPGs slowing down the heart rate by exciting the vagus nerve in the expiratory phase. The artificial CPG oscillators appear to compete with respiration to synchronize with the heart beat.

Captions:

FIGURE 1: Modulating the heart beat with a mutually inhibitory neuron pair

(a) A decerebrated rat is placed in ice-chilled carbogenated Ringer solution. Electrodes are attached to the thoracic phrenic nerve (PN), the central vagus nerve (VN) to record inspiration patterns and vagus nerve activity respectively. The ventricular pressure (LVP) and electrocardiogram (ECG) are also recorded to monitor the heart output and the heart rate. A pre-amplifier stage magnifies the phrenic signal by 10,000. A second amplifier stage rectifies and smoothes the pre-amplified signal which produces quasi-rectangular voltage pulses during inspiration. The voltage gain of the second stage is used to fine tune the amplitude of phrenic pulses relative to the firing threshold of neuron 1 (N1). A differential transconductance amplifier is fitted in output of the second stage to convert the voltage pulses into current pulses that stimulate neuron 1. Neurons 1 and 2 are a mutually inhibitory pair of silicon neurons which oscillate out of phase with each other. The voltage oscillations of neuron 1 (resp. neuron 2) are used to stimulate the vagus nerve in-phase (resp. out-of phase) with the phrenic input. The PN, ECG, LVP and VN outputs are recorded by the 'spike2' data acquisition software with a sampling frequency of 5kHz.

(b) Hardware network of 6 NaKl neurons that interact through 30 gap junction synapses. Our experiments on rats use the left-most pair of neurons with 2 one-way synapses linking these neurons together. The oscilloscope screen shot shows 3 neurons competing through 6 mutually inhibitory synapses.

(c) Typical time series current data input to neuron 1. The respiration cycle shows is divided into three phases: the inspiration phase (t_1), the early expiration phase (t_2) and the late expiration phase (t_3).

FIGURE 2: Motor activity induced by stimulating the vagus nerve in the inspiration phase - t_1.

The vagus nerve is stimulated by neuron N1 (blue trace). The time series data of the electrocardiograpm (ECG), ventricular pressure (LVP), phrenic input (PN), central vagus output (VN) and the "membrane" voltages of artificial neurons 1 (N1) and 2 (N2) are plotted for 2 rats: (a) rat #1, (b) rat #2.

Modulation of sinus arrhythmia with CPG hardware

(a) Rat #1 breathes at constant intervals of ~4s. Stimulation of the vagus nerve in the inspiration phase (t_1) induces a strong modulation of the cardiac output in the early expiration phase (t_2). The interval between heart beats increases from $ISI_1 = 0.2$s in phases 1&3 to $ISI_2 = 0.4$s in phase 2. Meanwhile, the ventricular pressure increases by a factor of 2.1.

(b) Rat #2 has a variable respiration rate which we increase through injection of vasopressin. Here again, stimulation of the vagus nerve in phase 1 causes the ECG rate to slow down from phase 1&3 to phase 2. The interval between heart beats increases from $ISI_1 = 0.19$s to $ISI_2 = 0.34$s while the amplitude of LVP oscillations increases. Neurons N1 and N2 remains synchronized to respiration cycle even through the respiration rate changes.

FIGURE 3: Motor activity induced by stimulating the vagus nerve in the expiration phase - $t_2 + t_3$.

The vagus nerve is now stimulated by neuron N2 (blue trace) out of phase with the PN signal.

(a) Rat #1 – The artificial modulation of ventricular pressure is weak and irregular. It manifests as the heart missing a beat (second derivative curve) most often in phase 1 or 3. Neuro-stimulation by N2 remains synchronized out-of-phase during the vasopressin drive.

(b) Rat #2 – The artificially induced sinus arrhythmia is equally small when the experiment is repeated on the second rat.

FIGURE 4: Motor activity induced by stimulating the vagus nerve in the early expiration phase - t_2.

The vagus nerve is stimulated by neuron N1 (blue trace) triggered by the central vagus nerve.

(a) Rat #2 - The firing threshold is set at the level of the VN peak producing a narrow spike burst at the beginning of phase 2. Virtually no sinus arrhythmia is reported.

(b) Rat #2 – The firing threshold is set at a lower level causing wider spike bursts that overlap regions 1 and 2. Strong sinus arrhythmia is observed with a tripling of the LVP amplitude and a doubling of the interval of the heart beat from 0.15s to 0.33s.

FIGURE 5: Motor activity induced by stimulating the vagus nerve in the late expiration phase - t_3.

The vagus nerve is stimulated by neuron N2 (blue trace) delayed by time τ.

(a) Rat #2 - A small delay τ stimulates the vagus nerve over the full length of the late expiration phase. Moderate sinus arrhythmia is induced the interval between heart beats increasing from $ISI_2 = 0.2$ in phase 2 to $ISI_3 = 0.27$s over intervals 3 and 1.

(b) Rat #2 - A longer delay τ is used to excite a fraction of the late expiratory phase (t_3). The resulting sinus arrhythmia is much weaker and hard to quantify.

FIGURE 6: Natural sinus arrhythmia in Rat #2. The feedback loop from the network is disconnected.

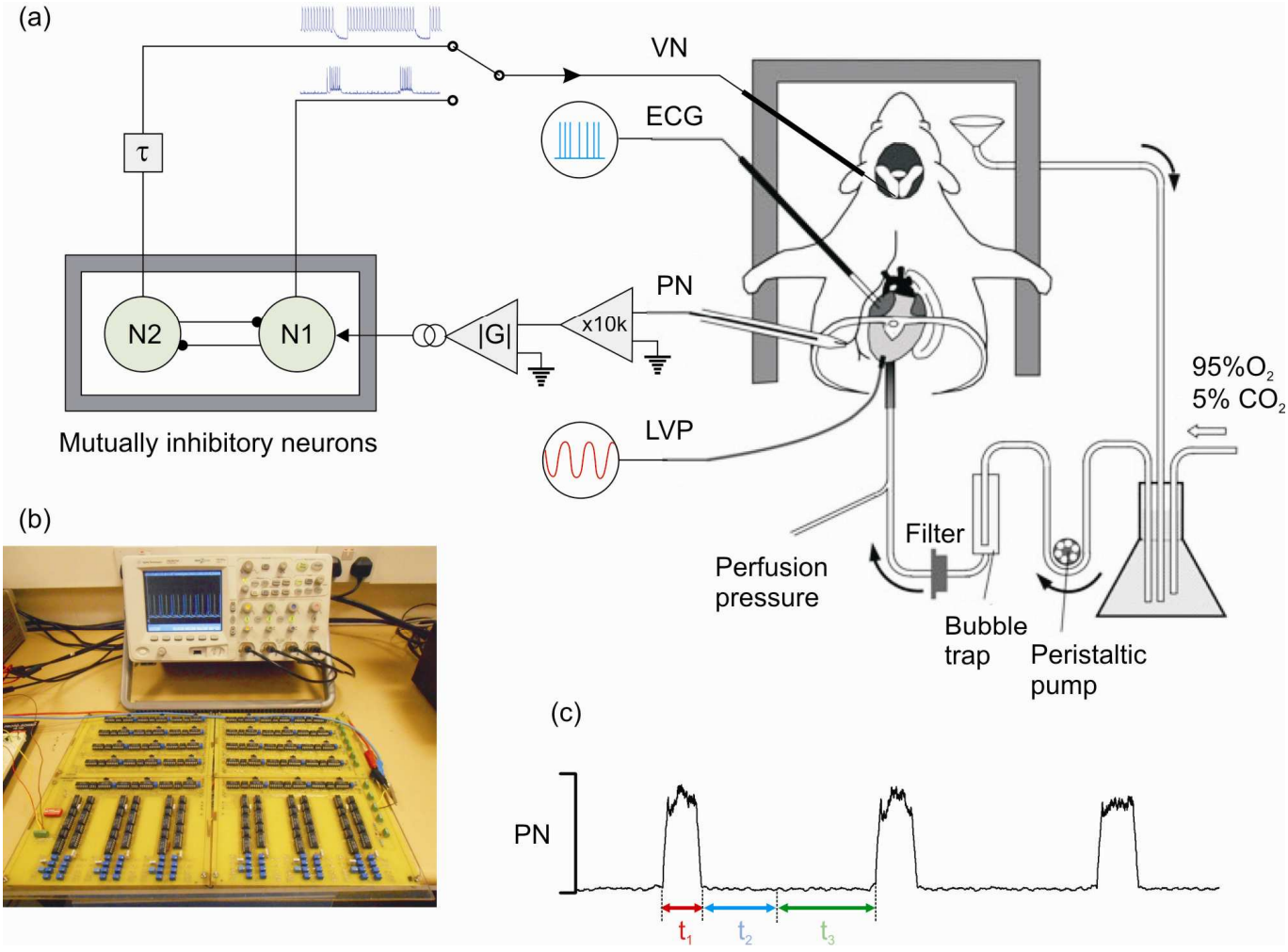
(a)
VN
ECG
τ
PN
N2
N1
|G|
x10k
Mutually inhibitory neurons
LVP
95%O2
5% CO2
Filter
Perfusion
pressure
Bubble
trap
Peristaltic
pump
(b)
(c)
PN
t1
t2
t3

Figure 1

(a)

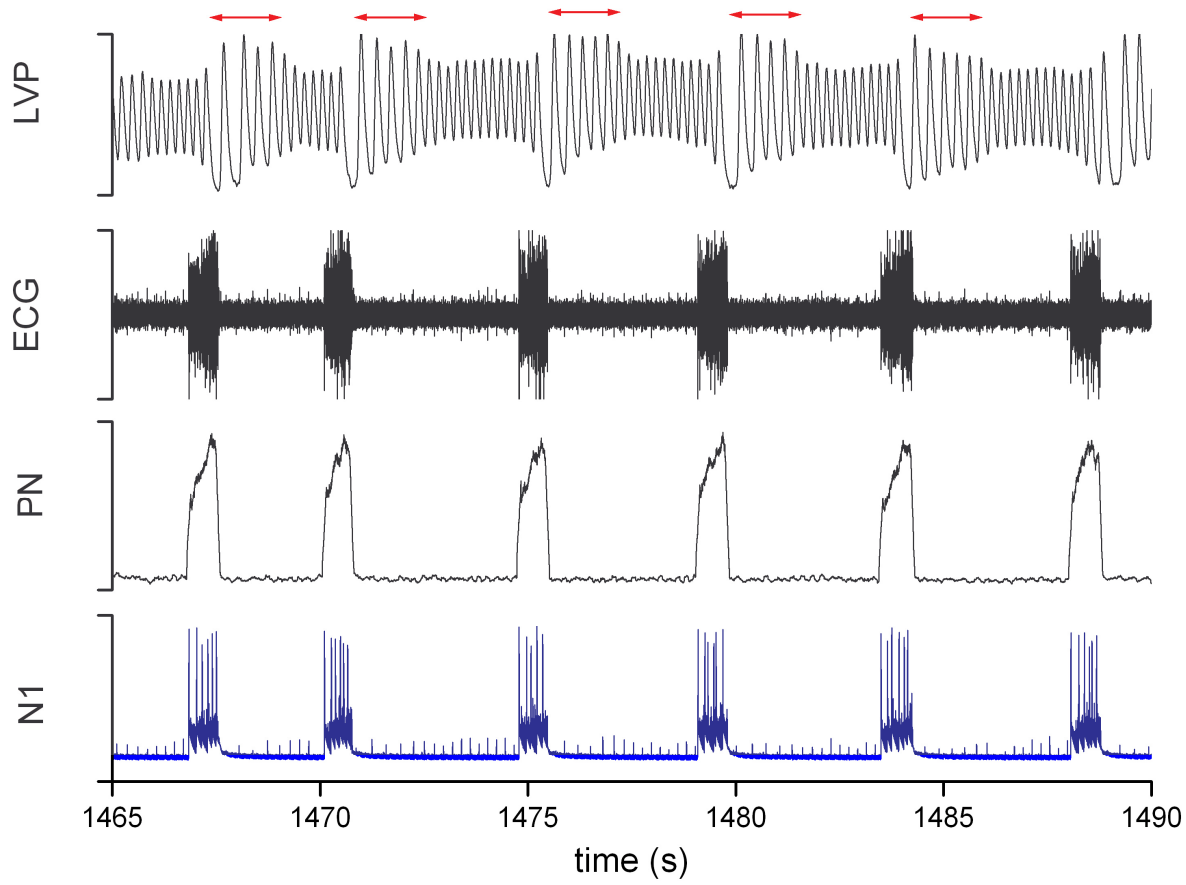
LVP
ECG
PN
N1
1465
1470
1475
1480
1485
1490
time (s)

(b)

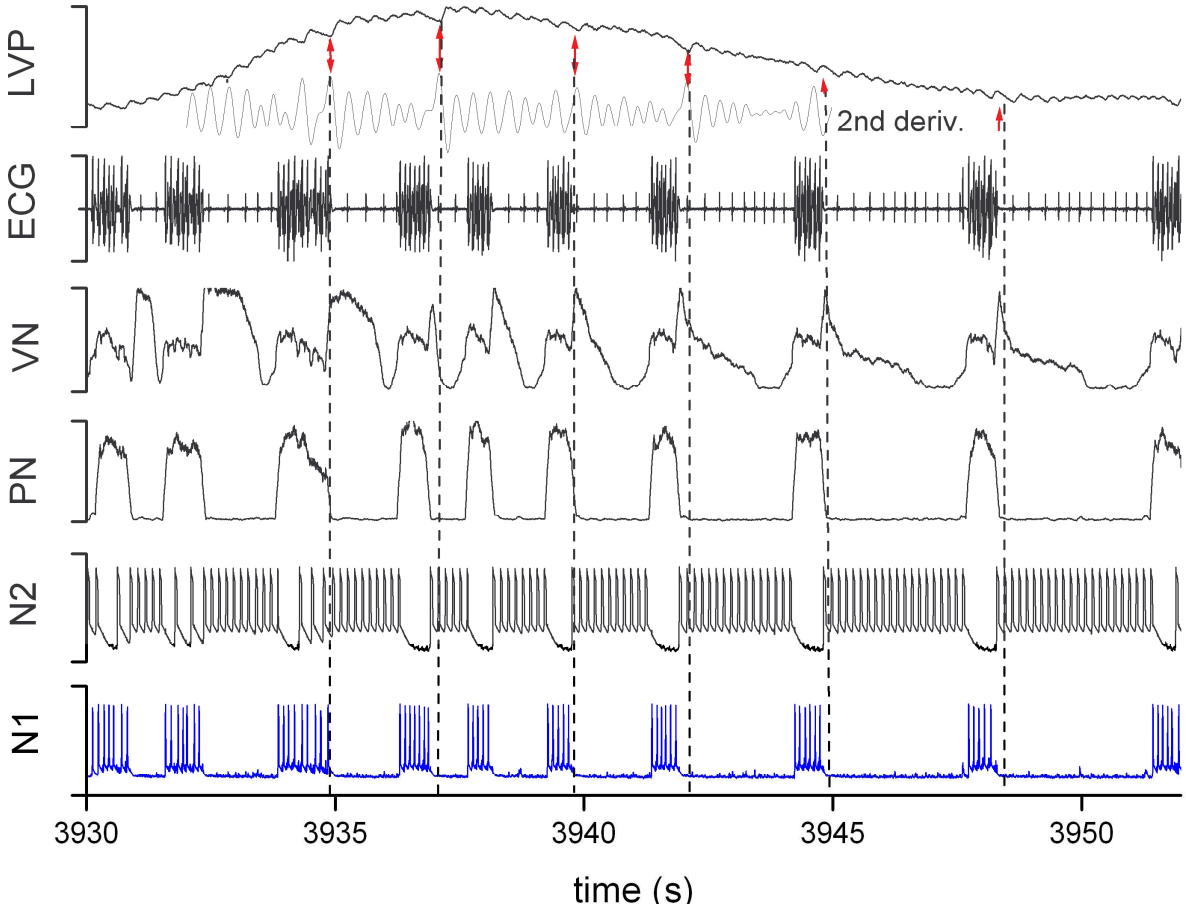
LVP
2nd deriv.
ECG
VN
PN
N2
N1
3930
3935
3940
3945
3950
time (s)

Figure 2

(a)

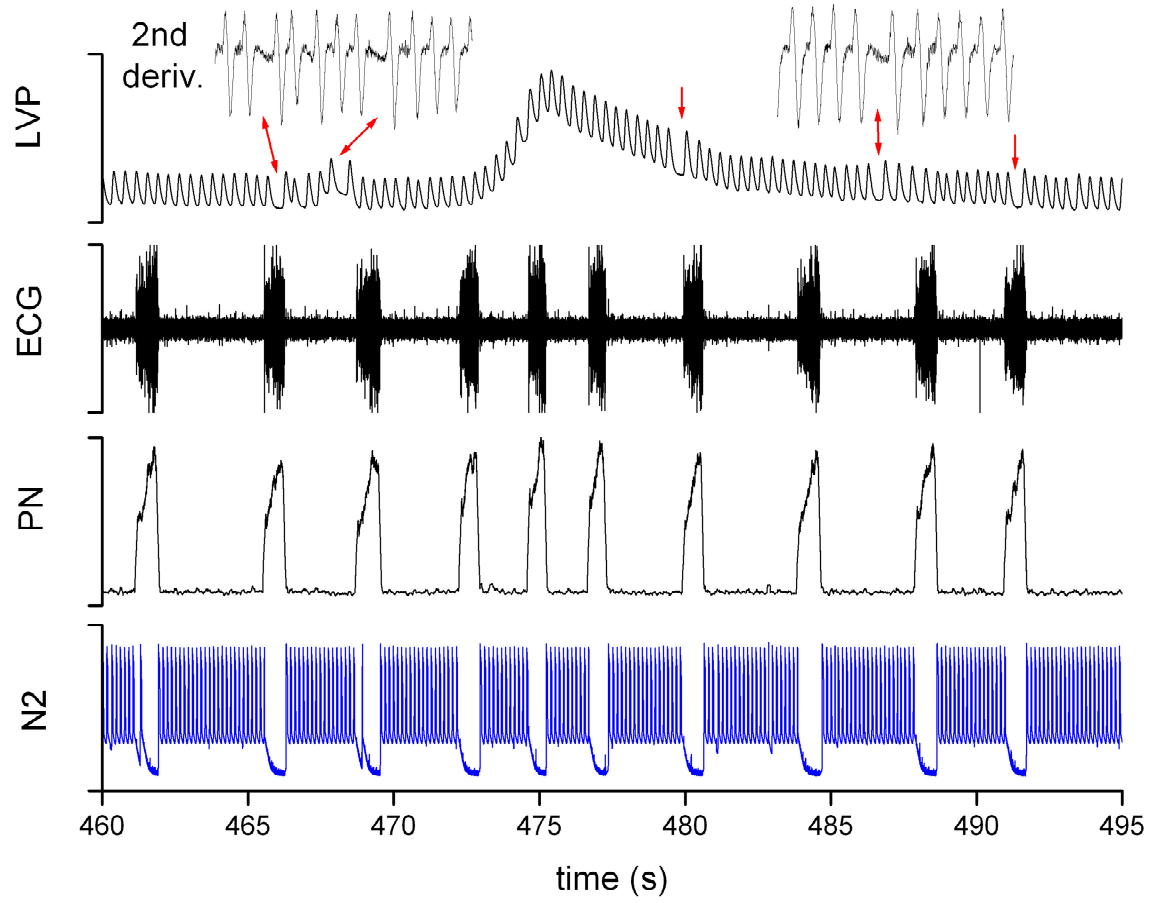
2nd
deriv.
LVP
ECG
PN
N2
460
465
470
475
480
485
490
495
time (s)

(b)

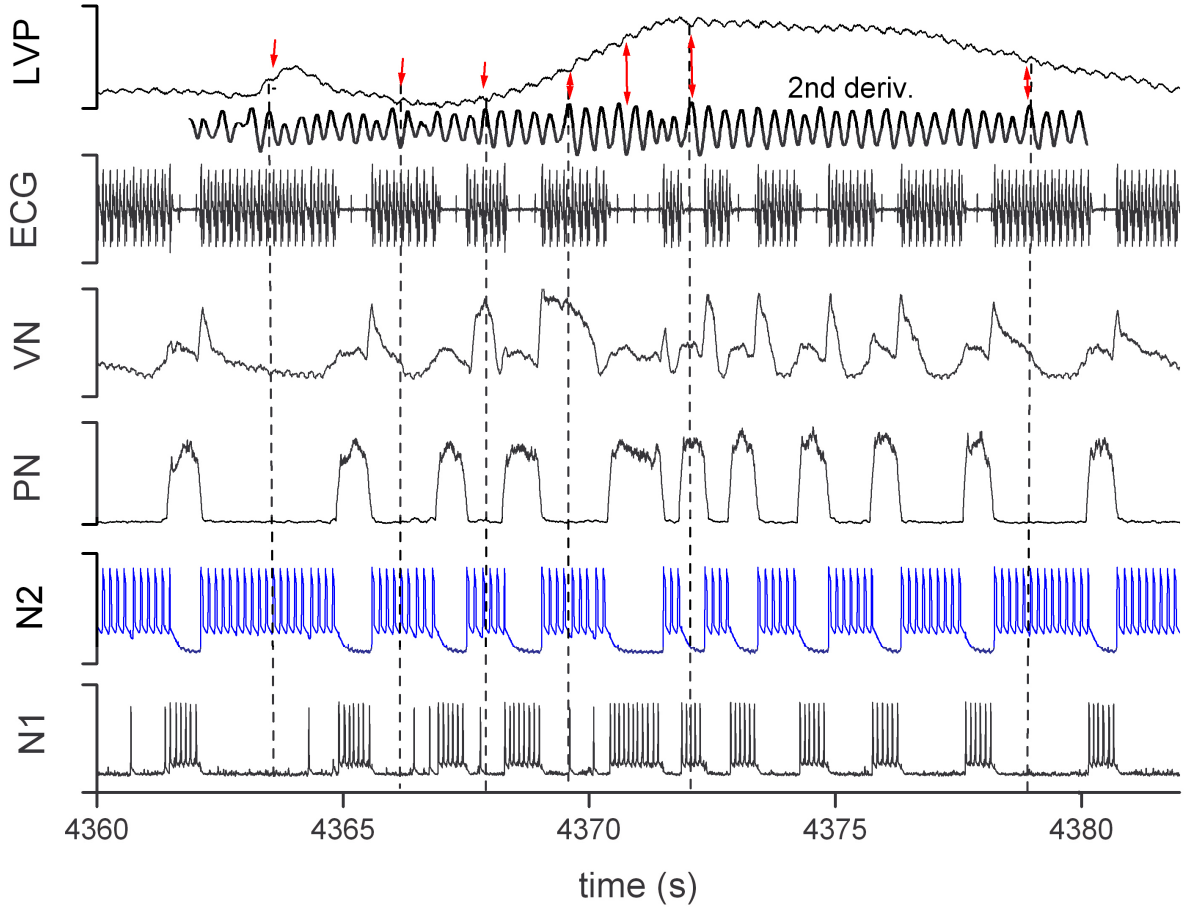
LVP
2nd deriv.
ECG
VN
PN
N2
N1
4360
4365
4370
4375
4380
time (s)

Figure 3

(a)

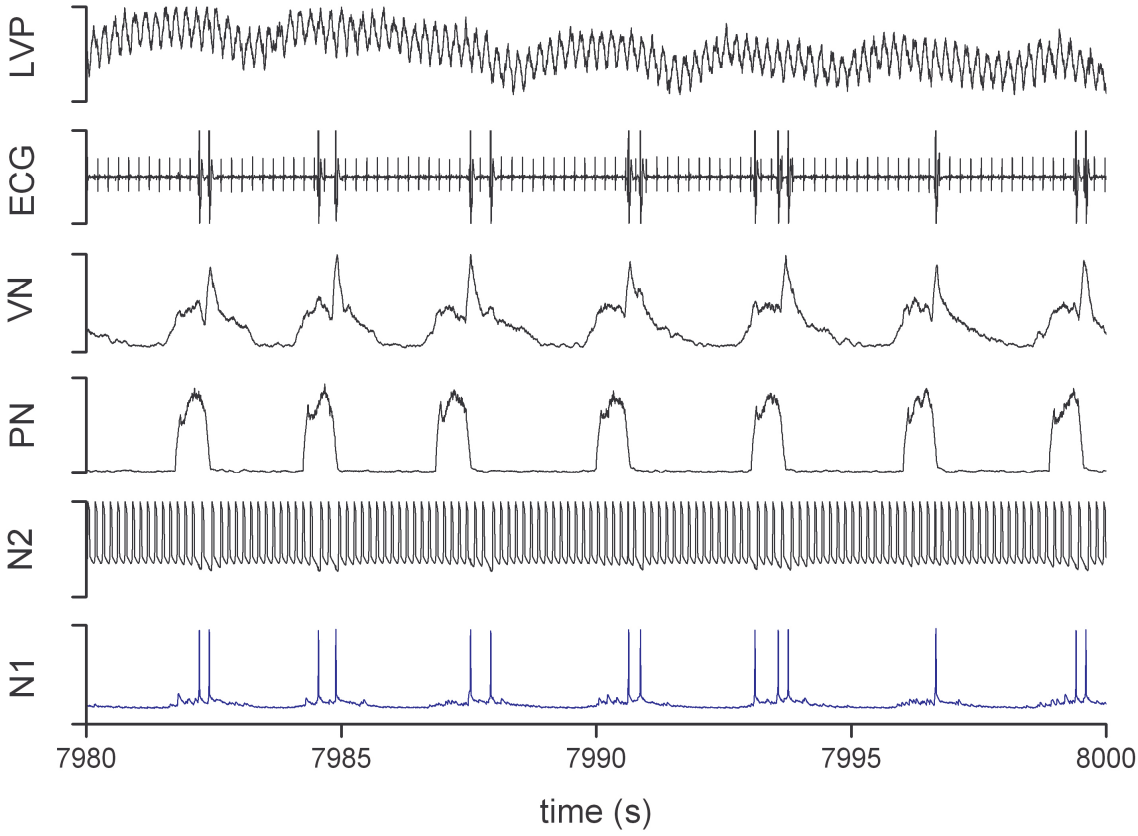
LVP
ECG
VN
PN
N2
N1
7980
7985
7990
7995
8000
time (s)

(b)

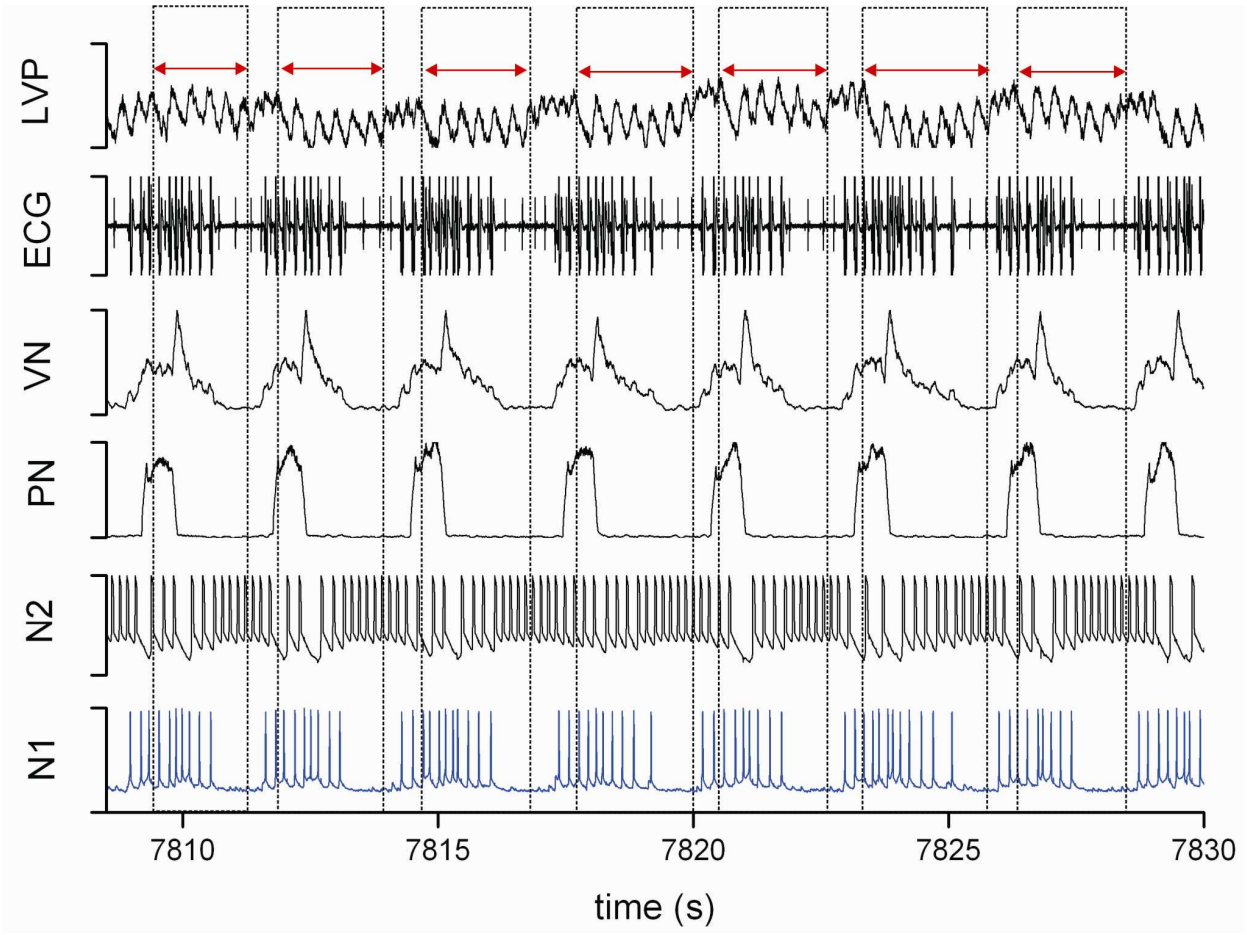
LVP
ECG
VN
PN
N2
N1
7810
7815
7820
7825
7830
time (s)

Figure 4

(a)

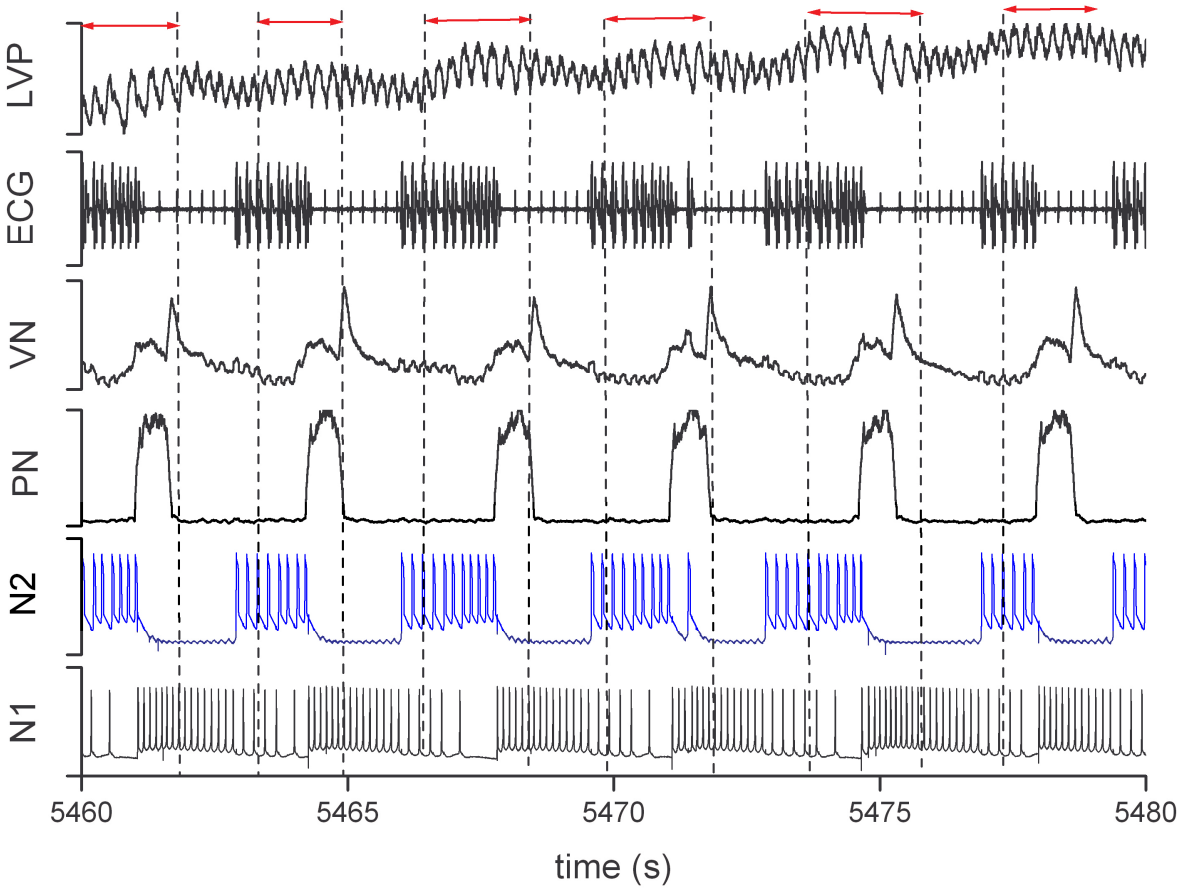
LVP
ECG
VN
PN
N2
N1
5460
5465
5470
5475
5480
time (s)

(b)

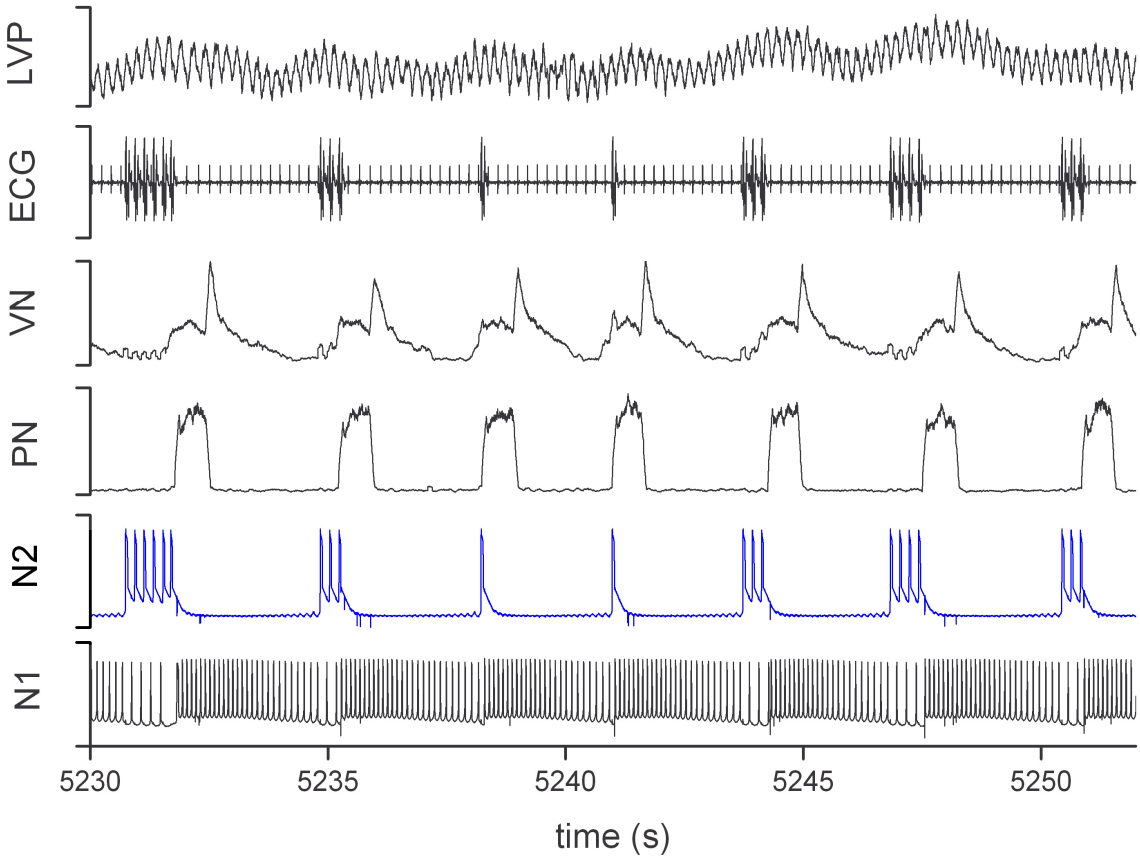
LVP
ECG
VN
PN
N2
N1
5230
5235
5240
5245
5250
time (s)

Figure 5

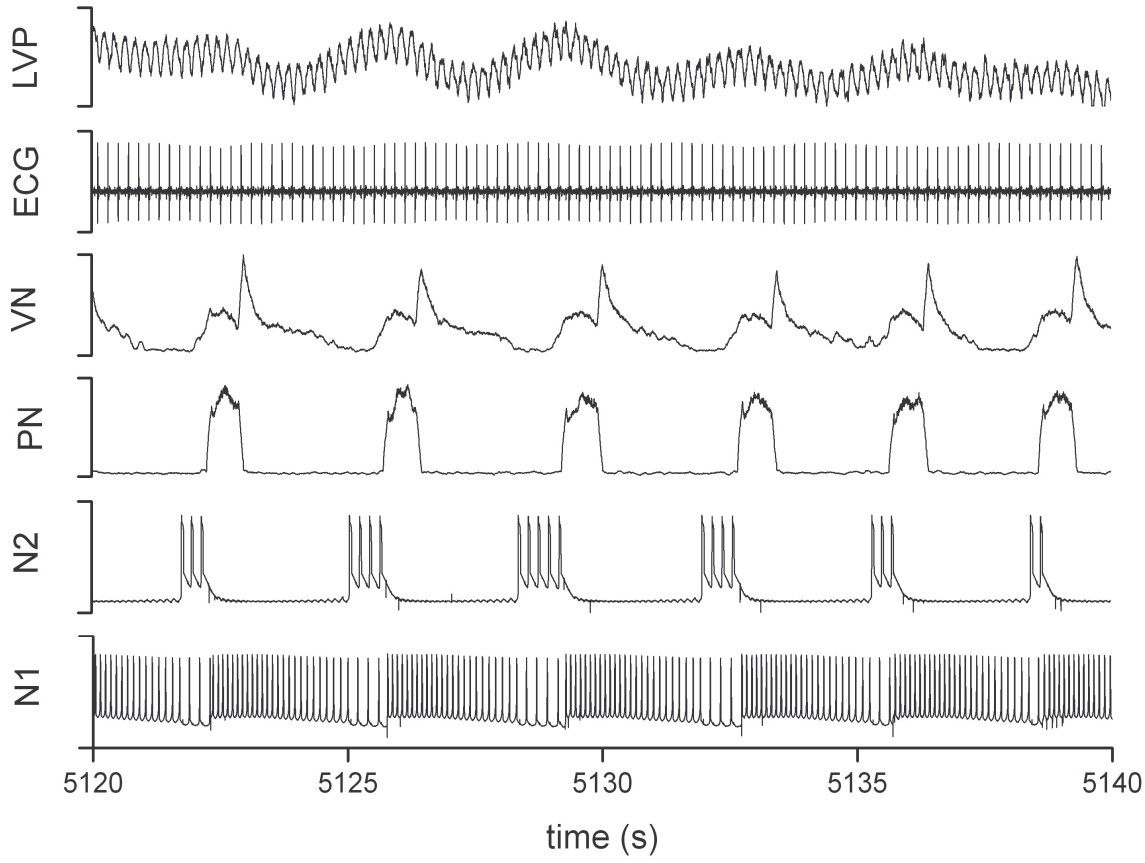

Figure 6

References:

Abarbanel HDI, Brown R, Sidorowich JJ & Tsimring LS (1993). The analysis of observed chaotic data in physical system. *Rev. Mod. Phys.* **65**, 1331-1392.

Abdala APL, Rybak IA, Smith JC & Paton JFR (2009). Abdominal expiratory activity in the rat brainstem –spinal cord *in situ*: patterns, origins and implications for respiratory rhythm generation. *J. Physiol.* **587.14**, 3539-3559.

Baekey DM, Molkov YI, Paton JFR, Rybak IA, Dick TE (2010). Effect of baroreceptor stimulation on the respiratory pattern: Insights into respiratory-sympathetic interactions. *Resp. Physiol. & Neurobiol.* **174**, 135-145.

Ben-Tal A, Shamailov SS & Paton JFR (2012). Evaluating the physiological significance of respiratory sinus arrhythmia: looking beyond ventilation-perfusion efficiency. *J. Physiol.* **590.8**, 1989-2008.

Champagnat J, Morin-Surun MP, Fortin G & Thoby-Brisson M (2009). Developmental basis of the rostro-caudal organization of the brainstem respiratory rhythm generator. *Phil. Trans. Soc. B* **364**, 2469-2476.

Cui Y, Wei Q, Park H & Lieber CM (2001). Nanowire nanosensors for highly selective detection of biological and chemical species. *Science* **293**, 1289-1292.

Daun S, Rubin JE & Rybak IA (2009). Control of oscillation periods and phase durations in half-center central pattern generators: a comparative mechanistic analysis. *J. Comput. Neurosci.* **27**, 3-36.

Elson RC, Selverston AI, Huerta R, Rulkov NF, Rabinovich MI & Abarbanel HDI (1998). Synchronous behavior of two coupled biological neurons. *Phys. Rev. Lett.* **81**, 5692-5695.

Fortuna MG, West GH, Stornetta RL & Guyenet PG (2008). Bötzinger expiratory-augmenting neurons and the parafacial respiratory group. *The J Neurosci.* **28**, 2506-2515.

Fortuna MG, Stornetta RL, West GH & Guyenet PG (2009). Activation of the retrotrapezoid nucleus by posterior hypothalamic stimulation, *J. Physiol.* **587**, 5121-5138.

Fromherz P (2002). Electrical interfacing of nerve cells and semiconductor chips. *ChemPhysChem* **3**, 276-284.

Fromherz P, Offenhäusser A, Vetter T, Weis J (1991). A neuron-silicon junction: A Retzius cell of the Leech on an insulated-gate field-effect transistor. *Science* **252**, 1290-1293.

Hess LH, Jansen M, Maybeck V, Moritz VH, Seifert M, Stutzmann M, Sharp ID, Offenhäusser A & Garrido JA (2011). Graphene transistor arrays for recording action potentials from electrogenic cells. *Adv. Mat.* **23** 5045-5049.

Jalil S, Belykh I & Shilnikov A (2010). Fast reciprocal inhibition can synchronize bursting neurons. *Phys. Rev. E* **81**, R045201.

Kristan WB Jr, Calabrese RL & Friesen WO (2005). Neuronal control of leech behavior. *Prog. Neurobiol.* **76**, 279-327.

Landa PS & Rosenblum MG (1995). Modified Mackey-Glass model of respiration control. *Phys. Rev. E* **52**, R36 (1995).

Mahowald M & Douglas R (1991). A silicon neuron. *Nature* **354**, 515-518.

Marder E, Bucher D, Schulz DJ & Taylor AL (2005). Invertebrate central pattern generator moves along. *Curr. Biol.* **15**, R685-R699.

Marder E & Calabrese RL (1996). Principle of rhythmic motor pattern generation. *Physiol. Rev.* **76**, 687-717.

Meliza D, Nogaret A, Toth BA, Kostuk M, Abarbanel HDI, Margoliash D (2012), Parameter extraction and predictive modelling of neurons in the songbird high vocal centre, *Neuron* (submitted)

Molkov YI, Abdala APL, Bacak BJ, Smith JC, Paton JFR & Rybak IA (2010). Late-expiratory activity: Emergence and interactions with the respiratory CPG. *J. Neurophysiol.* **104**, 2713-2729.

Nakamura Y & Katakura N (1995). Generation of masticatory rhythm in the brainstem. *Neurosci. Research* **23**, 1-19.

Nalivaiko E, Antunes VR & Paton JFR (2009). Control of cardiac contractility in the rat working heart-brainstem preparation. *Exp. Physiol.* **95**, 107-119.

Norris BJ, Weaver, AL, Morris, LG, Wenning A., Garcia PA & Calabrese RL (2006). A central pattern generator producing alternative outputs: Temporal pattern or premotor activity. *J. Neurophysiol.* **96**, 309-326.

Nicholls JG & Paton JFR (2009). Brainstem: neural networks vital for life. *Phil. Trans. Roy. Soc. B* **364**, 2447-2451.

Olypher A, Cymbalyuk G & Calabrese RL (2006). Hybrid systems-analysis of the control of burst duration by low-voltage-activated calcium current in leech heart interneurons. *J. Neurophysiol.* **96**, 2857-2867.

Patolsky F, Timko BP, Yu G, Fang Y, Greytak AB, Zheng G & Lieber CM (2006). Detection, stimulation, and inhibition of neuronal signals with high-density nanowire transistor arrays. *Science* **313**, 1100.

Pinto RD, Elson RC, Szücs A, Rabinovich MI, Selverston AI & Abarbanel HDI (2001). Extended dynamic clamp: controlling up to four neurons using a single desktop computer and interface. *J. Neurosci. Meth.* **108**, 39-48.

Rabinovich MI, Varona P, Selverston AI & Abarbanel HDI (2006). Dynamical principles in neuroscience. *Rev. Mod. Phys.* **78**, 1213-1265.

Rabinovich M, Volkovskii, Lecanda P, Huerta R, Abarbanel HDI & Laurent G (2001). Dynamical encoding by networks of competing neuron groups: Winnerless competition. *Phys. Rev. Lett.* **87**, 068102.

Rosenblum MG, Cimponeriu L, Bezerianos A, Patzak A, Mrowka R (2001). Identification of coupling direction. *Phys .Rev. E* **65**, 041909.

Rubin JE, Shevtsova NA, Ermentrout GB, Smith JC & Rybak IA (2009). Multiple rhythmic states in a model of the respiratory central pattern generator. *J. Neurophysiol*. **101**, 2146-2165.

Rulkov NF, Sushchik MM, Tsimring LS & Abarbanel HDI (1995). Generalized synchronization of chaos in directionally coupled chaotic systems. *Phys. Rev. E* **51**, 980 (1995).

Samardak A, Nogaret A, Janson NB, Balanov AG, Farrer I & Ritchie DA (2009). Noise controlled signal transmission in a multithread semiconductor neuron. *Phys. Rev. Lett.* **102**, 226802.

Schäfer C, Rosenblum MG, Abel H-H, Kurths J (1999). Synchronization in the human cardiorespiratory system. *Phys. Rev. E* **60**, 857.

Selverston AI (2010). Invertebrate central pattern generator circuits. *Phil. Trans. R. Soc. B* **365**, 2329-2345.

Shiba K, Nakazawa K, Ono K & Umezaki T (2007). Multifunctional laryngeal premotor neurons: Their activities during breathing, coughing sneezing and swallowing. *J.Neurosci.* **27**, 5156-5162.

Shilnikov A, Calabrese RL & Cymbalyuk G (2005). Mechanism of bistability: Tonic spiking and bursting in a neuron model. *Phys. Rev. E* **71**, 056214.

Smith JC, Abdala APL, Koizumi H, Rybak IA & Paton JFR (2007). Spatial and functional architecture of the mammalian brain stem respiratory network: a hierarchy of three oscillatory mechanisms. *J. Neurophysiol.* **98**, 3370-3397.

Sorensen M, De Weerth S, Cymbalyuk G & Calabrese RL (2004). Using a hybrid neural system to reveal regulation of neural network activity by an intrinsic current. *The J. of Neurosci.* **24**, 5427-5438.

Taylor BE & Lukowiak K (2000). The respiratory central pattern generator of *Lymnaea*: a model, measured and malleable. *Resp. Physiol.* **122**, 197-207 (2000).

Varona P, Torres JJ, Abarbanel HDI, Rabinovich MI & Elson RC (2001). Dynamics of two electrically coupled chaotic neurons: Experimental observations and model analysis. *Biol Cybern.* **84**, 91-101.

Zheng G, Patolsky F, Cui Y, Wang WU & Lieber CM (2005). Multiplexed electrical detection of cancer markers with nanowire sensor arrays. *Nature Biotech.* **23**, 1294-1301.